



Palladium(II) and platinum(II) complexes of a new imineoxime ligand – Structural, spectroscopic and DFT/time-dependent (TD) DFT studies

Yunus Kaya^{a,*}, Ceyda Icel^a, Veysel T. Yilmaz^a, Orhan Buyukgungor^b

^a Department of Chemistry, Faculty of Arts and Sciences, Uludag University, 16059 Bursa, Turkey

^b Department of Physics, Faculty of Arts and Sciences, Ondokuz Mayıs University, 55139 Samsun, Turkey

ARTICLE INFO

Article history:

Received 17 September 2013

Received in revised form

18 November 2013

Accepted 5 December 2013

Keywords:

Imineoxime

Coordination compound

Crystal structure

DFT calculation

ABSTRACT

A new imineoxime compound, (1*E*,2*E*)-[(2-hydroxyethyl)imino]-2-phenyl-ethanal oxime (heipeoH) and its palladium(II) and platinum(II) complexes ([M(heipeo)₂]) have been synthesized and characterized by elemental analysis, IR, NMR, UV–vis, mass spectra and X-ray diffraction. The geometry of heipeoH was optimized by both B3LYP with 6-311++G(d,p) and LANL2DZ basis sets, while the molecular structures of both complexes obtained from X-ray diffraction were compared with the optimized geometries using the B3LYP with the LANL2DZ basis set. In addition, the quantum chemical studies of title compounds have been carried out to correlate geometry and spectroscopic properties such as electronic, vibrational and NMR chemical shifts. The atomic charges of the title compounds were calculated by natural bond orbital (NBO) analysis.

© 2013 Elsevier B.V. All rights reserved.

1. Introduction

Imineoximes include both oxime and imine groups in their structure. They have been extensively used in analytical chemistry for detection and separation of metal ions [1–5], due to the fact that imineoximes act as chelating ligands via the imine and oxime groups [6–8]. Moreover, some oximes and their complexes have been reported to have significant biochemical activities [9–17]. Specifically palladium(II) and platinum(II) complexes of oximes received considerable attention due to their DNA binding affinities [18–20].

In the last decade, density functional theory (DFT) was used extensively in the modeling of oximes and their metal complexes [21–28]. Literature surveys have revealed the high degree of accuracy of DFT methods in reproducing the experimental values in terms of geometry, dipole moment, electronic transitions, vibrational frequency and NMR chemical shifts [21,29–40]. Recently, we reported a combined experimental and theoretical study of an imineoxime, namely (1*E*,2*E*)-phenyl-[(1-phenylethyl)imino]-ethanal oxime (ppeioH) [41] and its palladium(II) [42] and platinum(II) [43] complexes. The *cisoid* and *transoid* conformations of *E*- and *Z*-isomers of ppeioH have been identified [41]. At the same time, the

hydrolysis mechanism of ppeioH in solution has been clarified [43]. In addition, the electronic, vibrational and NMR spectra of ppeioH and its palladium(II) complex have been characterized using DFT.

As a part of our work, in this paper, we report the synthesis of a new imineoxime, (1*E*,2*E*)-[(2-hydroxyethyl)imino]-2-phenyl-ethanal oxime (heipeoH) and its palladium(II) and platinum(II) complexes, namely [Pd(heipeo)₂] and [Pt(heipeo)₂]. Both metal complexes were obtained as single crystals, while all attempts for the crystallization of the heipeoH ligand failed. The theoretical studies including electronic, vibrational and NMR spectra and NBO charges have been performed by DFT, and the calculations were correlated with the experimental values. The results show that these calculations are valuable for providing insight into molecular properties of the imineoxime compound and its complexes.

2. Experimental and calculations

2.1. Instrumentation

The elemental analyses (C, H and N) were performed using a EuroEA 3000 CHNS elemental analyser. Mass spectrum of heipeoH was obtained using an Agilent-LCMS spectrometer. UV–vis spectra were measured on a Perkin–Elmer Lambda 35 UV/vis spectrophotometer using 1×10^{-4} M EtOH solution in the 200–800 nm range. IR spectra were recorded on a Thermo Nicolet 6700 FT-IR spectrophotometer as KBr (in the frequency range 4000–

* Corresponding author. Tel.: +90 224 2941738; fax: +90 224 2941898.

E-mail address: ykaya@uludag.edu.tr (Y. Kaya).

400 cm^{-1}) and CsI (in the frequency range 400–250 cm^{-1}) pellets. ^1H NMR (400 MHz) and ^{13}C NMR (100 MHz) spectra were recorded on a Varian Mercury plus spectrometer in $\text{DMSO}-d_6$ and CDCl_3 . TMS was used as an internal standard.

2.2. Synthesis of ligand and its complexes

(1*E*,2*E*)-[(2-hydroxyethyl)imino]-2-phenyl-ethanal oxime (heipeoH) was prepared by refluxing a mixture of a solution containing isonitrosoacetophenone (inapH) (0.750 g, 5 mmol) in 10 mL EtOH and a solution containing monoethanolamine (0.310 g, 5 mmol) in 5 mL EtOH. The reaction mixture was refluxed for 3 h. The reaction mixture yields a polycrystalline white powder. Yield 87%. M.p. 134.1 °C; Anal. Calc. for $\text{C}_{10}\text{H}_{12}\text{N}_2\text{O}_2$ (192.2 g mol^{-1}): C, 62.49; H, 6.29; N, 14.57. Found: C, 61.80; H, 6.16; N, 14.36%, ESI-MS, (m/z) = 192.6 [M^+].

In synthesis of $[\text{Pd}(\text{heipeo})_2]$ and $[\text{Pt}(\text{heipeo})_2]$ complexes, a solution of a heipeoH (0.192 g, 1 mmol) in EtOH (30 mL) was added drop wise to a solution of $\text{Na}_2[\text{PdCl}_4]$ (0.147 g, 0.5 mmol) and $\text{K}_2[\text{PtCl}_4]$ (0.208 g, 0.5 mmol) in water (10 mL). After the addition of NaOH (0.040 g, 1 mmol) in 2 mL water, the mixtures were stirred for 4 h at ambient temperature. The volumes of the solutions were reduced to 10–15 mL under vacuum and then the resulting precipitate was filtered, and dried in air. X-ray quality orange and yellow crystals of the palladium(II) and orange crystals of the platinum(II) complexes were obtained by the slow evaporation of the EtOH solutions at ambient temperature within two days. For $[\text{Pd}(\text{heipeo})_2]$ complex; Yield 76%. M.p. 202–212 °C (decomp.); Anal. Calc. for $\text{C}_{20}\text{H}_{22}\text{N}_4\text{O}_4\text{Pd}$ (488.8 g mol^{-1}): C, 49.14; H, 4.54; N, 11.46. Found: C, 48.96; H, 4.32; N, 11.43%. For $[\text{Pt}(\text{heipeo})_2]$ complex; Yield 73%. M.p. 259–264 °C (decomp.); Anal. Calc. for $\text{C}_{20}\text{H}_{22}\text{N}_4\text{O}_4\text{Pt}$ (577.5 g mol^{-1}): C, 41.60; H, 3.84; N, 9.70. Found: C, 41.52; H, 3.69; N, 9.66%.

2.3. Crystal structure determination

The intensity data of the palladium(II) and platinum(II) complexes were collected using a STOE IPDS 2 diffractometer with graphite-monochromated MoK_α radiation ($\lambda = 0.71073 \text{ \AA}$). The structures were solved by direct methods and refined on R^2 with the SHELX-97 program [44]. All non-hydrogen atoms were found from the difference Fourier map and refined anisotropically. All hydrogen atoms were positioned geometrically and refined by a riding model. The details of data collection, refinement and crystallographic data are summarized in Table S1.

2.4. Computational details

All calculations were conducted using DFT with the Becke–Lee–Yang–Parr functional (B3LYP) method [45] as implemented in the GAUSSIAN 03 program package [46]. In the first step of the calculation, to elucidate conformational features of the heipeoH, the selected degrees of torsional freedom, $\text{T}(\text{N}2-\text{C}7-\text{C}8-\text{N}1)$ and $\text{T}(\text{C}7-\text{N}2-\text{C}9-\text{C}10)$, were varied from -180° to $+180^\circ$ in every 10° and the potential energy curve (PES) was obtained with the B3LYP/6-31G(d) level of theory. In potential energy curve, the stationary points were confirmed by the frequency analysis as minima with all real frequency and with no imaginary frequency implying no transition state. For the lowest energy conformer, the geometric structure was reoptimized in ground state at the DFT level of theory by using 6-311++G(d,p) and LANL2DZ basis sets. Ground state geometry optimization of the palladium(II) and platinum(II) complexes were started from the X-ray experimental atomic positions and fully optimized at B3LYP and LANL2DZ level. The harmonic vibrational frequencies of the heipeoH were calculated using the

B3LYP/6-311++G(d,p) basis set, while those of the complexes were calculated at B3LYP/LANL2DZ basis set.

The computed frequency values contain systematic errors [47] and therefore, we have used scaling factors: In the calculations made by the B3LYP/6-311++G(d,p) basis set, scaling factors 0.958 [48] and 0.978 [49] were used for 4000–1700 cm^{-1} and 1700–400 cm^{-1} ranges, respectively. In the calculations by the B3LYP/LANL2DZ basis set, a modified wavenumber-linear-scaling (WLS) approach [50,51] was employed after completing the vibrational mode assignments for palladium(II) and platinum(II) complexes. This method was derived by determining the best-fit linear function between the experimental and theoretical data. The resulting functions are shown in Eqs. (1)–(4).

For the palladium(II) complex:

$$y = 1.0165x - 240.91 \quad (R^2 = 0.99) \quad \text{for } 4000 - 1700 \text{ cm}^{-1} \quad (1)$$

$$y = 1.0203x - 39.465 \quad (R^2 = 0.99) \quad \text{for } 1700 - 250 \text{ cm}^{-1} \quad (2)$$

For the platinum(II) complex:

$$y = 1.0109x - 228.040 \quad (R^2 = 0.99) \quad \text{for } 4000 - 1700 \text{ cm}^{-1} \quad (3)$$

$$y = 1.0287x - 50.142 \quad (R^2 = 0.99) \quad \text{for } 1700 - 250 \text{ cm}^{-1} \quad (4)$$

The assignment of the calculated frequencies is aided by the animation option of GaussView 3.0 graphical interface for Gaussian programs, which gives a visual presentation of the shape of the vibrational modes [52]. Furthermore, theoretical vibrational spectra of the title compounds were interpreted by means of PEDs using VEDA 4 program [53].

^1H and ^{13}C NMR chemical shifts (δ_{H} and δ_{C}) of heipeoH and its complexes were calculated using the GIAO method [54] in DMSO and chloroform at the B3LYP/LANL2DZ level and using the TMS shielding calculated as a reference.

Transition energies and oscillator strengths for the electronic excitation of the first 12 singlet-to-singlet excited states of heipeoH and 48 singlet-to-singlet excited states of the metal complexes were calculated using time-dependent (TD) DFT at the B3LYP/LANL2DZ level. Each excited state was interpolated by a Gaussian convolution with the full width at half-maximum (fwhm) of 3000 cm^{-1} . In addition, the electronic absorption spectra were calculated in EtOH using the IEFPCM method. Orbital contribution was analyzed using GaussSum software [55].

Natural bond orbital (NBO) analysis for the title compounds have been obtained using the B3LYP/LANL2DZ basis set.

3. Results and discussion

3.1. Conformational analysis of heipeoH

The $\text{N}2-\text{C}7-\text{C}8-\text{N}1$ and $\text{C}7-\text{N}2-\text{C}9-\text{C}10$ dihedral angles are the most relevant for conformational flexibility for the heipeoH molecule (Fig. S1). Conformations of this molecule are also feasible depending on the orientation around $\text{C}7-\text{C}8$ and $\text{N}2-\text{C}9$ bonds. Conformational analysis was carried by the potential energy surface scan to find all possible conformers with B3LYP method using 6-31G(d) basis set. The potential energy surface of heipeoH is

shown in Fig. S2. All of the possible geometries of the conformers were optimized to find out the most stable configuration. The most stable conformer of heipeoH was then subjected to the geometrical optimization by B3LYP method using 6-311++G(d,p) and LANL2DZ basis sets to obtain geometrical parameters, vibrational frequencies, NMR, the atomic charges, electronic and thermodynamic properties. In the most stable conformer, the N2–C7–C8–N1 and C7–N2–C9–C10 dihedral angles were computed as -176.5 and -147.5° . An intramolecular hydrogen bond was formed between the hydrogen of the hydroxyethyl group and the nitrogen atom of the imine group. This hydrogen bonding further contributes to the stability of the conformer.

3.2. Description of the crystal structures of [Pd(heipeo)₂] and [Pt(heipeo)₂]

The molecular structures of [Pd(heipeo)₂] and [Pt(heipeo)₂] complexes are shown in Figs. 1 and 2, and the selected bond lengths and angles are listed in Table 1. The title complexes are isomorphous and crystallize in a triclinic space group $P\bar{1}$. Cocrystallization of two polymorphs of [Pd(heipeo)₂] was observed by the different colors and shapes of the crystals and were identified by X-ray measurements with C_1 and C_1 point groups. The polymorphism in the palladium(II) complex seems to be due to the orientation of the hydroxyethyl groups (Fig. 1). The C_1 polymorph of [Pd(heipeo)₂] and [Pt(heipeo)₂] are centrosymmetric and the metal ions lie on the inversion center. In addition, the two phenyl rings are coplanar in these complexes, while these aromatic rings form a dihedral angle of 66.66° in the palladium(II) complex with the C_1 point group. The Pd–N and Pt–N bond distances range from 2.025(3) to 2.059(3) Å and are typical for previously reported palladium(II) and platinum(II) complexes containing imineoximes or oximes [13,15,42,43,56–63].

The [Pd(heipeo)₂] (C_1) and [Pt(heipeo)₂] complexes are linked by strong intermolecular O–H...O hydrogen bonds involving the

hydroxyl hydrogen atom and the oxime O atom (Table 1). The hydrogen bonds result in a one-dimensional chain running along the b axis and these chains are held together by weak C–H...O hydrogen bonds involving the phenyl and aldehyde hydrogens, and the hydroxyl O atoms leading to a three-dimensional network. The polymorphism affects the packing of the molecules in [Pd(heipeo)₂] (C_1) and contrary to the C_1 polymorph, this complex is stabilized by two O–H...O hydrogen bonds involving hydroxyl hydrogen atom and the oxime O atom and hydroxyl hydrogen atom and the hydroxyl O atom (Table 1).

3.3. Optimized geometry

The optimized parameters (bond lengths and bond angles) of heipeoH, obtained using the B3LYP/6-311++G(d,p) and LANL2DZ basis sets are listed in Table 2. The optimized structure of heipeoH together with the atomic numbering is shown in Fig. S1. For the complexes, the selected structural parameters obtained experimentally and calculated theoretically using the B3LYP/LANL2DZ method are tabulated in Table 1. The most important bonds of imineoxime compounds are C=N(imine) and C=N(oxime). These bond lengths of heipeoH were calculated 1.305 and 1.302 Å, respectively. On the other hand, the C=N bond lengths were obtained between 1.325 and 1.331 Å in the palladium(II) and platinum(II) complexes. These results show that both C=N bonds of the ligand weaken upon complexation. The optimized parameters by DFT show a small difference from those obtained by X-ray diffraction. The largest differences between the experimental observations and those obtained from the theoretical calculations are 0.166 Å in the O–H bond length and 2.8° in the C7–N2–C9 bond angle. When the X-ray structures of the complexes are compared to its optimized counterparts (see Fig. S3), slight conformational discrepancies are observed between them. The most remarkable discrepancy exists in the orientation of the hydroxyethyl group in [Pt(heipeo)₂] and the C_1 polymorph of [Pd(heipeo)₂] with the C9–

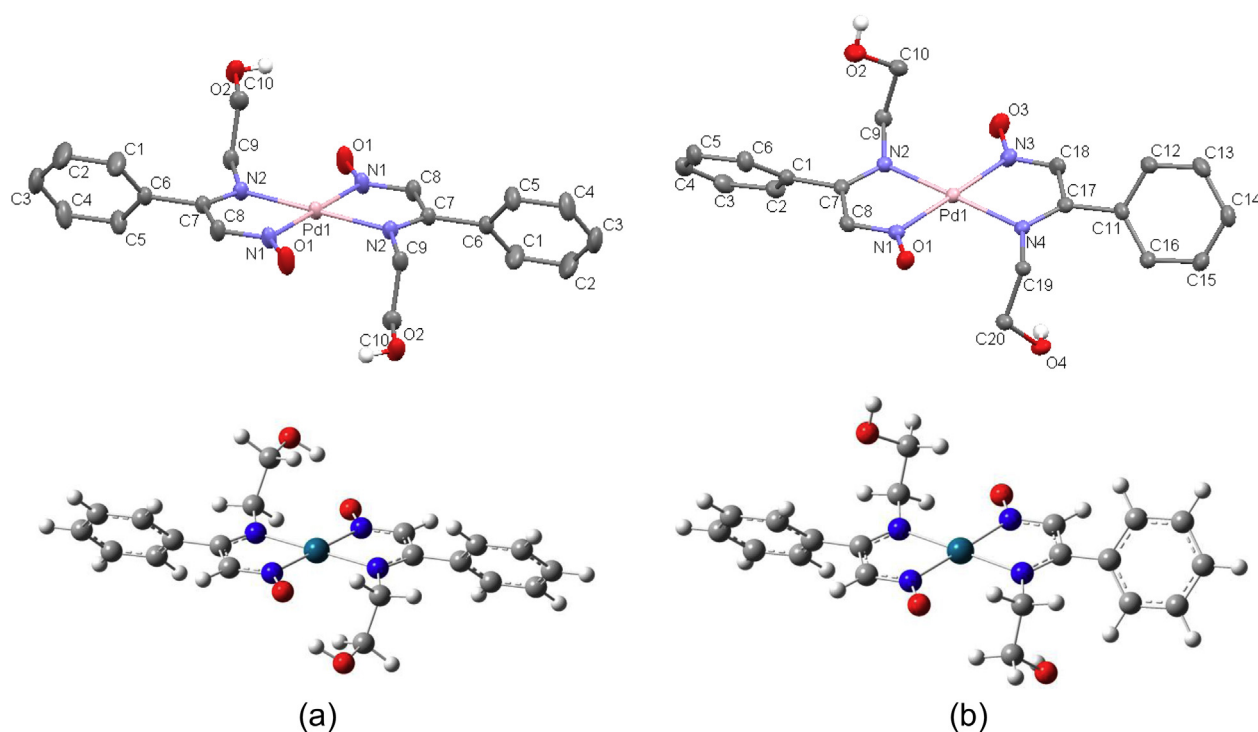


Fig. 1. X-ray and optimized structures of [Pd(heipeo)₂], (a) C_1 point group, (b) C_1 point group.

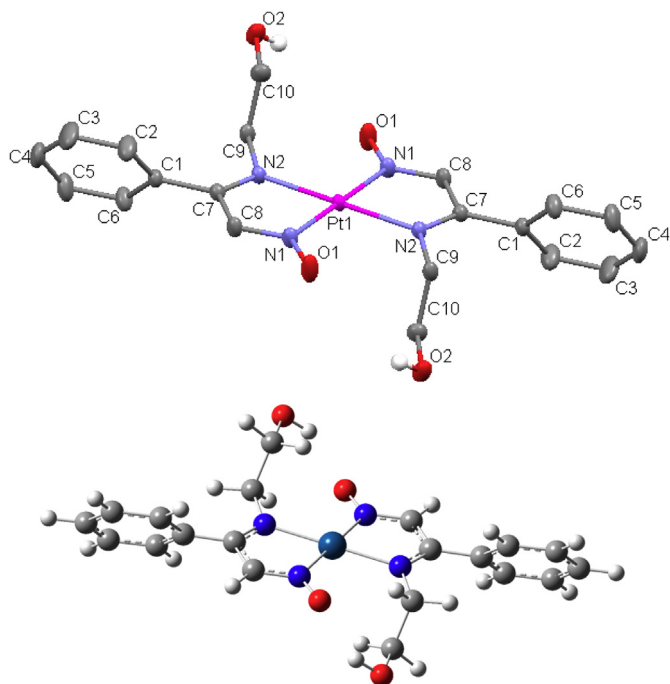


Fig. 2. X-ray and optimized structures of [Pt(heipeo)₂].

C10–O2–H torsion angles of -60.1 and -96.7° , respectively. The corresponding torsion angles were calculated as ca. -66.5° .

3.4. IR Spectra

The harmonic vibrational frequencies for heipeoH were calculated by using DFT method at 6-311++G(d,p) basis set, while those of [Pd(heipeo)₂] and [Pt(heipeo)₂] complexes were calculated by

Table 1
Selected bond lengths (Å) and angles ($^\circ$) for [Pd(heipeo)₂] and [Pt(heipeo)₂].

	Experimental	LANL2DZ	Experimental	LANL2DZ
<i>[Pd(heipeo)₂], C_i</i>				
Pd1–N1	2.039(3)	2.088	N2–Pd1–N1	100.9(11)
Pd1–N2	2.045(3)	2.084	N1–Pd1–N1	180.0(1)
			N1–Pd1–N2	79.1(11)
			N2–Pd1–N2	180.0(1)
<i>[Pd(heipeo)₂], C_i</i>				
Pd1–N1	2.046(3)	2.080	N1–Pd1–N2	79.5(13)
Pd1–N2	2.043(3)	2.083	N2–Pd1–N3	99.9(14)
Pd1–N3	2.035(3)	2.077	N3–Pd1–N4	79.4(13)
Pd1–N4	2.059(3)	2.091	N4–Pd1–N1	101.2(13)
			N1–Pd1–N3	179.1(15)
			N2–Pd1–N4	178.1(11)
<i>[Pt(heipeo)₂]</i>				
Pt1–N1	2.025(18)	2.071	N1–Pt1–N2	78.8(7)
Pt1–N2	2.028(18)	2.071	N1–Pt1–N1	180.0(8)
			N2–Pt1–N1	101.2(7)
			N2–Pt1–N2	180.0(8)
Hydrogen bonds ^a				
D–H...A	D–H (Å)	H...A (Å)	D...A (Å)	D–H...A ($^\circ$)
<i>[Pd(heipeo)₂], C_i</i>				
O2–H2...O4 ⁱ	0.82	2.03	2.831(4)	165.5
O4–H2...O3 ⁱⁱ	0.82	1.90	2.683(4)	160.8
<i>[Pd(heipeo)₂], C_i</i>				
O2–H2...O1 ⁱⁱⁱ	0.82	1.98	2.763(4)	159.3
<i>[Pt(heipeo)₂]</i>				
O2–H2...O1 ^{iv}	0.82	2.20	2.755(3)	124.8

^a Symmetry codes: (i) $x, y, -1 + z$; (ii) $1 - x, -y, 1 - z$; (iii) $x, y + 1, z$; (iv) $x, y - 1, z$.

Table 2
Selected geometric parameters of heipeoH.

	6-311++G(d,p)	LANL2DZ
Bond length (Å)		
C1–C2	1.393	1.406
C2–C3	1.394	1.409
C3–C4	1.394	1.408
C4–C5	1.393	1.406
C5–C6	1.399	1.414
C1–C6	1.399	1.413
C6–C7	1.499	1.503
C7–C8	1.475	1.482
C9–C10	1.530	1.541
C8–N1	1.276	1.302
C7–N2	1.281	1.305
C9–N2	1.455	1.474
N1–O1	1.394	1.447
O1–H	0.964	0.982
C10–O2	1.419	1.455
O2–H	0.966	0.984
Bond angle ($^\circ$)		
C1–C2–C3	120.2	120.3
C2–C3–C4	119.8	119.7
C3–C4–C5	120.1	120.1
C4–C5–C6	120.4	120.6
C1–C6–C7	120.6	120.8
C2–C1–C6	120.3	120.4
C7–C8–N1	120.9	121.8
C8–N1–O1	111.3	110.0
C6–C7–N2	125.9	126.2
C6–C7–C8	119.0	119.9
N2–C9–C10	108.3	107.2
C7–N2–C9	122.2	123.8
C9–C10–O2	111.7	110.6

using DFT at LANL2DZ basis set. The corresponding frequencies along with the assignments and intensities are given in Tables S2 and S3, while the observed and calculated vibrational spectra are given in Fig. S4. The calculated frequencies with the intensity less than 5 were not taken into consideration. It can be seen that, the experiment has a better correlation with the calculations. In the IR spectra of heipeoH, the O–H stretching vibrations of the oxime and hydroxyethyl groups were calculated at 3661 and 3618 cm^{-1} , respectively, while observed at 3218 and 3429 cm^{-1} , respectively [41,64,65]. The deviation between the experimental and calculated values seems to be significant for the hydroxyl groups frequencies with a difference of 443 and 189 cm^{-1} . Due to the nature of this vibration mode, its frequency is very sensitive to the crystalline state, in which the hydrogen bonding interactions involving this group are present as discussed above, and thus exhibits much larger deviation from the calculated values. At the same time, in the high wavenumber region of the spectra, the anharmonicity can explain substantial differences between the experimental and calculated values [66]. The experimental C=N bands were observed as sharp bands at 1624 cm^{-1} , which was computed at 1647 cm^{-1} [$\nu_{\text{CN}_{\text{imine}}}$ (63) + $\nu_{\text{CN}_{\text{oxime}}}$ (18)] and 1597 cm^{-1} , calculated as 1634 cm^{-1} [$\nu_{\text{CN}_{\text{oxime}}}$ (59) + $\nu_{\text{CN}_{\text{imine}}}$ (12)] cm^{-1} [30,39,41]. In addition, strong characteristic absorption due to N–O stretching vibration is observed at 985 cm^{-1} , and calculated at 973 cm^{-1} [ν_{NO} (64) + δ_{CN} (11)] [27,29,39,41,64,65]. In the IR spectra of [Pd(heipeo)₂] and [Pt(heipeo)₂], the $\nu(\text{O–H})$ of the oxime group was not observed, due to the fact that the imineoxime loses this hydroxyl proton upon complexation. The frequency of the hydroxyethyl group was observed at 3483 cm^{-1} in [Pd(heipeo)₂] and 3430 cm^{-1} in [Pt(heipeo)₂], while calculated at 3429 and 3420 cm^{-1} , respectively. The imine group (C=N) of [Pd(heipeo)₂] and [Pt(heipeo)₂] was calculated at 1583 (%57 CN) and 1580 (%51 CN) cm^{-1} , observed at 1623 and 1624 cm^{-1} [22]. The oxime group (C=N) of both complexes was observed at 1597 cm^{-1} , while calculated at ca. 1505 cm^{-1} [67,68]. It is interesting that the frequencies of the imine

and oxime groups did not change in the complexes compared to the free ligand. A substantial change is also observed in the N–O stretching, which appears at 985 cm^{-1} in the free heipeoH. The N–O absorptions were occurred at 1217 cm^{-1} (calcd. 1234 cm^{-1}) for $[\text{Pd}(\text{heipeo})_2]$ and 1214 cm^{-1} (calcd. 1236 cm^{-1}) for $[\text{Pt}(\text{heipeo})_2]$, indicating an increase in the double bond character of the NO bond upon complexation [69,70]. Vibrational modes in the low wave-number region of the spectra contain $\nu(\text{M}-\text{N})$ stretching together with contributions of other several modes. The $[\text{Pd}(\text{heipeo})_2]$ and $[\text{Pt}(\text{heipeo})_2]$ show two bands at $531\text{--}255$ and $534\text{--}251\text{ cm}^{-1}$, respectively, which can be attributed to $\nu(\text{M}-\text{N})$ (calcd. $530\text{--}215\text{ cm}^{-1}$) [42,43].

3.5. NMR Spectra

Experimental ^1H and ^{13}C NMR spectra of heipeoH were taken in $\text{DMSO-}d_6$ solvent, while those of $[\text{Pd}(\text{heipeo})_2]$ and $[\text{Pt}(\text{heipeo})_2]$ were measured in CDCl_3 . The chemical shifts are given in Table 3, while the NMR spectra obtained by the DFT method at the GIAO/B3LYP/LANL2DZ level with TMS as a reference are illustrated in Figs. S5–S7. The numbering of the atoms is the same as in Figs. 1 and 2 and S1. In ^1H NMR spectra of heipeoH, the resonances centered at ca. 7.82, 3.58 and 3.21 ppm are assigned to the aldehyde proton of the oxime group and the methylene protons of the hydroxyethyl group. These signals were calculated as 9.17, 3.02 and 2.85 ppm. The corresponding protons in the complexes were observed at 7.90/7.67, 3.87/4.12 and 3.69/3.83 ppm (Pd complex/Pt complex), which are calculated at 7.82/7.91, 3.41/4.12 and 2.49/3.83 ppm, respectively. The deuterium exchangeable protons of the hydroxyimino and hydroxyethyl groups of the ligand show characteristic chemical shifts and appear at a singlet at 11.70 and 4.57 ppm, respectively. They are calculated as 9.17 and 2.89 ppm. The hydroxyethyl proton of both complexes was observed at ca. 4.35 ppm, while calculated at ca. 2.95 ppm. The multiple signals between 7.17 and 7.51 ppm represent the aromatic protons of the phenyl groups of both ligands and its complexes, and they were calculated at 7.05–8.48 ppm. The ^1H NMR spectra of the ligand and its complexes are not correlated well with the calculated spectrum,

Table 3
Experimental and calculated ^1H and ^{13}C NMR chemical shifts of heipeoH, $[\text{Pd}(\text{heipeo})_2]$ and $[\text{Pt}(\text{heipeo})_2]$ (ppm).^a

	HeipeoH		$[\text{Pd}(\text{heipeo})_2]$		$[\text{Pt}(\text{heipeo})_2]$	
	Exp.	Calcd.	Exp.	Calcd.	Exp.	Calcd.
^1H NMR						
O1–H	11.70	9.17	–	–	–	–
C8–H	7.82	8.48	7.90	7.82	7.67	7.91
C1–H	7.43–7.17	7.22	7.45–7.22	7.12	7.51–7.35	7.05
C2–H		7.47		7.50		7.50
C3–H		7.52		7.56		7.57
C4–H		7.45		7.50		7.50
C5–H		7.13		7.12		7.15
O2–H	4.57	2.89	4.38	2.91	3.42	2.99
C9–H ₂	3.58	3.02	3.87	3.41	4.12	3.55
C10–H ₂	3.21	2.85	3.69	2.49	3.83	2.60
^{13}C NMR						
C7	166.26	166.38	175.91	170.43	177.72	168.28
C8	152.55	158.73	145.69	150.30	146.52	149.72
C6	135.07–	127.08	131.70–	124.95	131.31–	124.46
C1	128.22	124.85	127.21	123.20	127.46	123.41
C2		122.03		123.53		123.66
C3		123.34		125.13		125.17
C4		122.03		123.26		123.27
C5		124.10		124.47		124.52
C9	56.21	55.68	50.87	48.66	52.32	50.09
C10	61.45	60.48	63.35	59.59	63.38	59.72

^a In CDCl_3 with TMS as a reference.

since imineoximes exhibit a number of conformers and calculations are referred to the static molecule [71,72]. However, in the case ^{13}C NMR spectra, the experimental chemical shifts are in accordance with the calculated values. In the computed ^{13}C spectrum of the ligand, the signal at 166.26 ppm belongs to the imine C atom and was calculated as 166.38 ppm, while the signal at 152.55 ppm is assigned to the C=N–O group of heipeoH (calcd. 158.73 ppm). The signals between 126.2 and 135.1 ppm are assigned to the phenyl carbon atoms of heipeoH. These signals were calculated between 122.03 and 127.08 ppm. The chemical shifts of the C9 and C10 atoms of heipeoH are observed at 56.21 and 61.45 ppm, respectively and were calculated at 55.68 and 60.48 ppm. In the case of metal complexes, the carbon of the imine group experiences deshielding, while that of the oxime group exhibits shielding compared those of the ligand.

3.6. Electronic absorption spectra

The UV–vis absorption spectra of heipeoH and its complexes were measured in EtOH. The absorption bands of the compounds were assigned based on TDDFT. The calculated excited states, absorption bands, oscillator strengths (f_{os}), transition configuration and their assignments are given in Table 4 together with the experimental bands. Several absorption bands were observed in the spectra of heipeoH, and its complexes (Fig. S8). Relative percentages of atomic contributions to the lowest unoccupied and highest occupied molecular orbitals were placed in Table S4. The assignment of the calculated transitions to the experimental bands is based on the criterion of the energy and oscillator strength of the calculated transitions. The absorption bands of the heipeoH appear at around 227 and 286 nm. The absorption band at 227 nm can be mainly assigned to a superposition of three calculated bands between 218 and 249 nm. We ascribe the absorption band at 286 nm to the calculated transition at 275 nm with oscillator strength of 0.0629. Both transitions can be ascribed to the $\pi \rightarrow \pi^*$ transition [41].

In the $[\text{Pd}(\text{heipeo})_2]$ complex, LUMO and LUMO + 1 are constructed mainly from the π^* orbital of imineoxime (74 and 70%, respectively) and LUMO + 2 consists of %36 π^* orbital of imineoxime and 45% the d-orbitals of metal, while LUMO + 3 consists of %79 π^* orbital of the phenyl ring. The higher occupied molecular orbitals (HOMOs) can be described as π orbitals of imineoxime (from HOMO to HOMO – 2), π orbitals of phenyl (from HOMO – 4 to HOMO – 7) and the metal d-orbitals (from HOMO – 10 to HOMO – 14). On the other hand, in the $[\text{Pt}(\text{heipeo})_2]$ complex, the LUMO and LUMO + 1 orbitals consist of the π^* orbital of imineoxime (72 and 70%, respectively), while LUMO + 2 is composed mainly of the metal d-orbitals (41%) and π^* orbital of imineoxime (30%). In addition, LUMO + 3 to LUMO + 5 can be described as π^* orbital of phenyl group. The HOMO orbitals consist mainly of the π orbitals of imineoxime and the phenyl group (from HOMO to HOMO – 16, except HOMO – 4, HOMO – 11 and HOMO – 12). The HOMO – 4, HOMO – 11 and HOMO – 12 orbitals have 40, 68 and 61% of the metal d-orbital character (Table S4). Moreover, the isodensity plots for the HOMOs and LUMOs orbitals of $[\text{Pd}(\text{heipeo})_2]$ and $[\text{Pt}(\text{heipeo})_2]$ complexes are shown in Fig. 3.

Based on TDDFT calculations of $[\text{Pd}(\text{heipeo})_2]$ and $[\text{Pt}(\text{heipeo})_2]$ complexes, the intense high-energy absorptions were observed at λ_{max} of 262 and 295 nm, respectively. The experimental band of $[\text{Pd}(\text{heipeo})_2]$ complex at 262 nm can be mainly assigned to a superposition of four calculated bands between 261 and 276 nm, and can be assigned to ligand to ligand charge transfer (LLCT), ligand to metal charge transfer (LMCT) and metal to ligand charge transfer (MLCT) transitions. On the other hand, the experimental band of $[\text{Pt}(\text{heipeo})_2]$ complex at 295 nm can be assigned to a superposition

Table 4
Experimental and calculated electronic transitions, oscillator strengths and their assignments for heipeoH, [Pd(heipeo)₂] and [Pt(heipeo)₂].^a

Exp. (nm)	ϵ	Calcd. (nm)	f_{os}	Major contribution (Cl coeff)	Character
<i>HeipeoH</i>					
286	0.121	275	0.0629	H – 3 → L (%46)	$\pi(\text{phen./imineoxime}) \rightarrow \pi^*(\text{imineoxime})$
227	3.569	249	0.1127	H – 4 → L (%83)	$\pi(\text{hydroxyethyl}) \rightarrow \pi^*(\text{imineoxime})$
		240	0.1514	H – 5 → L (%53)	$\pi(\text{oxime}) \rightarrow \pi^*(\text{imineoxime})$
		218	0.0956	H → L + 1 (%40)	$\pi(\text{phen./})/\pi(\text{imineoxime}) \rightarrow \pi^*(\text{phen.})$
				H – 1 → L + 1 (%31)	$\pi(\text{phen./hydroxyethyl}) \rightarrow \pi^*(\text{phen.})$
<i>[Pd(heipeo)₂]</i>					
397	0.883	446	0.0300	H → L (%70)	$d(\text{Pd})/\pi(\text{imineoxime}) \rightarrow \pi^*(\text{imineoxime})$
306	3.182	366	0.0602	H – 1 → L + 2 (%52)	$\pi(\text{imineoxime}) \rightarrow d(\text{Pd})/\pi^*(\text{imineoxime})$
				H – 2 → L + 1 (%27)	$\pi(\text{oxime}) \rightarrow \pi^*(\text{imineoxime})$
		347	0.3322	H – 4 → L (%83)	$\pi(\text{phen.}) \rightarrow \pi^*(\text{imineoxime})$
		343	0.1018	H – 2 → L + 2 (%63)	$\pi(\text{oxime}) \rightarrow d(\text{Pd})/\pi^*(\text{imineoxime})$
		318	0.0614	H – 10 → L (%48)	$d(\text{Pd})/\pi(\text{oxime}) \rightarrow \pi^*(\text{imineoxime})$
262	4.699	276	0.0620	H – 5 → L + 2 (%36)	$\pi(\text{phen.}) \rightarrow d(\text{Pd})/\pi^*(\text{imineoxime})$
		266	0.2492	H – 7 → L + 2 (%18)	$\pi(\text{phen.}) \rightarrow d(\text{Pd})/\pi^*(\text{imineoxime})$
				H – 5 → L + 2 (%15)	
		263	0.0935	H – 7 → L + 2 (%62)	$\pi(\text{phen.}) \rightarrow d(\text{Pd})/\pi^*(\text{imineoxime})$
		261	0.0967	H – 14 → L (%59)	$d(\text{Pd}) \rightarrow \pi^*(\text{imineoxime})$
		244	0.1141	H → L + 3 (%74)	$d(\text{Pd})/\pi(\text{imineoxime}) \rightarrow \pi^*(\text{phen.})$
<i>[Pt(heipeo)₂]</i>					
479	0.540	503	0.0300	H → L (%83)	$d(\text{Pt})/\pi(\text{imineoxime}) \rightarrow \pi^*(\text{imineoxime})$
410	0.626	396	0.0300	H – 4 → L (%35)	$d(\text{Pt})/\pi(\text{phen.}) \rightarrow \pi^*(\text{imineoxime})$
				H – 1 → L + 1 (%17)	$\pi(\text{imineoxime}) \rightarrow \pi^*(\text{imineoxime})$
				H – 2 → L + 1 (%16)	$\pi(\text{oxime}) \rightarrow \pi^*(\text{imineoxime})$
362	1.388	368	0.6329	H – 4 → L (%57)	$d(\text{Pt})/\pi(\text{phen.}) \rightarrow \pi^*(\text{imineoxime})$
331	2.268	333	0.0676	H – 11 → L (%42)	$d(\text{Pt})/\pi(\text{oxime}) \rightarrow \pi^*(\text{imineoxime})$
				H – 8 → L (%24)	$\pi(\text{hydroxyethyl/oxime}) \rightarrow \pi^*(\text{imineoxime})$
295	2.818	314	0.1442	H – 12 → L (%39)	$d(\text{Pt}) \rightarrow \pi^*(\text{imineoxime})$
				H – 2 → L + 1 (%11)	$\pi(\text{oxime}) \rightarrow \pi^*(\text{imineoxime})$
		302	0.1403	H – 12 → L (%46)	$d(\text{Pt}) \rightarrow \pi^*(\text{imineoxime})$
				H – 11 → L (%18)	$d(\text{Pt})/\pi(\text{oxime}) \rightarrow \pi^*(\text{imineoxime})$
		286	0.0770	H – 5 → L + 1 (%79)	$\pi(\text{phen./hydroxyethyl}) \rightarrow \pi^*(\text{imineoxime})$
		253	0.1723	H → L + 3 (%86)	$d(\text{Pt})/\pi(\text{imineoxime}) \rightarrow \pi^*(\text{phen.})$
		243	0.1211	H → L + 5 (%51)	$d(\text{Pt})/\pi(\text{imineoxime}) \rightarrow \pi^*(\text{phen.})$
				H – 2 → L + 2 (%17)	$\pi(\text{oxime}) \rightarrow d(\text{Pt})/\pi^*(\text{imineoxime})$
		242	0.1395	H → L + 5 (%40)	$d(\text{Pt})/\pi(\text{imineoxime}) \rightarrow \pi^*(\text{phen.})$
				H – 16 → L (%14)	$\pi(\text{hydroxyethyl/phen.}) \rightarrow \pi^*(\text{imineoxime})$

^a ϵ = Molar absorption coefficient ($\times 10^4$, $\text{dm}^3 \text{mol}^{-1} \text{cm}^{-1}$), f_{os} = oscillator strength, H = highest occupied molecular orbital, L = lowest unoccupied molecular orbital, phen. = phenyl.

of three calculated bands at 286 ($f = 0.077$), 302 ($f = 0.140$) and 314 nm ($f = 0.144$), and can be attributed to the MLCT and LLCT transitions of $d(\text{Pt}) \rightarrow \pi^*(\text{imineoxime})$ and $\pi(\text{phen./hydroxyethyl}) \rightarrow \pi^*(\text{imineoxime})$. The other absorption band

observed at 306 nm in the [Pd(heipeo)₂] complex can be assigned to a superposition of four calculated bands between 318 and 366 nm with LLCT, MLCT and LMCT. The last experimental band at 397 nm (calcd. 446 nm) in the [Pd(heipeo)₂] complex resulted from HOMO to LUMO (70%). Thus this band is assigned to mixed LLCT and MLCT involving $d(\text{Pd})/\pi(\text{imineoxime}) \rightarrow \pi^*(\text{imineoxime})$ transition [42]. In the [Pt(heipeo)₂] complex, the absorption at 331 nm (calcd. 333 nm) originates from the transition between HOMO – 11 and LUMO (42%), HOMO – 8 and LUMO (24%). The absorption at 362 nm (calcd. 368 nm) is contributed by excitation from HOMO – 4 to LUMO. The lower energy transitions at 410 (calcd. 396 nm) and 479 nm (calcd. 503 nm) mainly originate from the electronic transition HOMO – 4 to LUMO and HOMO to LUMO, respectively. Finally, the absorptions of the platinum(II) complexes may be assigned to MLCT and LLCT transitions.

3.7. NBO atomic charges

Effective atomic charge calculations have an important role in the application of quantum chemical calculation to molecular system because of atomic charge changes effect dipole moment, molecular polarizability, electronic structure, acidity–basicity behavior and more a lot of properties of molecular systems. In addition, NBO charge calculations provide information about the electrons movement between ligand and metal atom. The NBO atomic charges [73,74] were calculated using the B3LYP/LANL2DZ basis set. The results are listed in Table 5. As can also be seen from

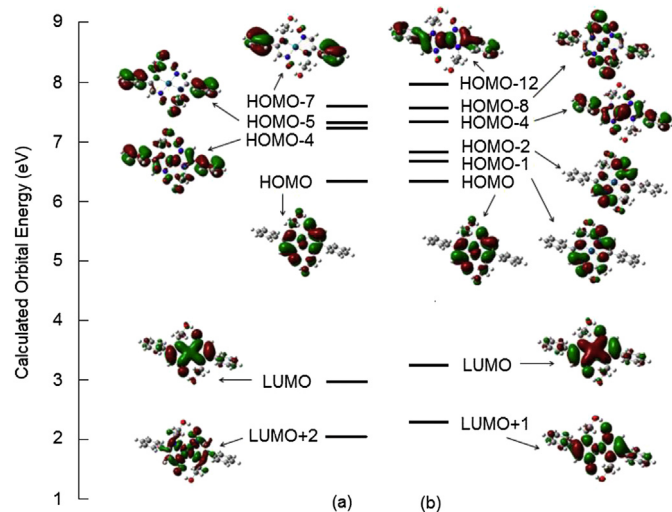


Fig. 3. Molecular orbital surfaces for the HOMOs and LUMOs orbitals of (a) Pd(heipeo)₂ and (b) [Pt(heipeo)₂].

Table 5
NBO charge distribution on main atoms of heipeoH and its complexes.

	HeipeoH	[Pd(heipeo) ₂], C ₁	[Pd(heipeo) ₂], C _i	[Pt(heipeo) ₂]
Pd/Pt	–	0.716	0.733	0.776
N _{oxime}	–0.149	–0.082, –0.081	–0.078	–0.090
N _{imine}	–0.627	–0.560, –0.544	–0.539	–0.547
O _{oxime}	–0.586	–0.460	–0.494	–0.499
O _{hydroxyethyl}	–0.794	–0.805, –0.808	–0.794	–0.791

NBO charge distribution, the binding sites of heipeoH are preferentially N(oxime) and N(imine) positions in favor to O(hydroxyethyl). The difference between the charge of the N(oxime) and N(imine) atoms in the complexes and in the free ligand can be taken into account as an approximation of the charge transfer from the ligand to metal. The values show that all complexes over these donor groups have a similar covalent contribution (between 0.059 and 0.071), whereas for the –OH groups, a covalent contribution is very little (between 0.003 and 0.011 values), which are an indicative evidence of the complex formation through the N(oxime) and N(imine) donor groups. Also, it can be seen from Table 5 that most of the positive charges are located on each metal atom, even though it is less than +2 required for Pd²⁺ and Pt²⁺ (the average value for all structures is between 0.716 and 0.776).

4. Conclusions

In this study, a new imineoxime compound (1E,2E)-(2-hydroxyethyl)imino-2-phenyl-ethanal oxime (heipeoH) and its palladium(II) and platinum(II) complexes, namely [Pd(heipeo)₂] and [Pt(heipeo)₂], have been synthesized and characterized by various techniques including elemental analysis, IR, NMR, UV–vis, mass spectra and X-ray diffraction. Conformational analysis was carried for heipeoH with B3LYP/6-31G(d) level, then the most stable conformer was determined. Its dihedral angles N2–C7–C8–N1 and C7–N2–C9–C10 were computed as –176.5° and –147.5°. X-ray crystallographic analysis of the [Pd(heipeo)₂] complex shows two polymorphs due to orientation of the hydroxyethyl groups. In both complexes, the palladium and platinum atoms are coordinated by two imineoxime ligands, behaving as a bidentate ligand. In order to study electronic, vibrational and NMR properties of the heipeoH, [Pd(heipeo)₂] and [Pt(heipeo)₂] complexes, the theoretical calculations were successfully performed by using DFT with the B3LYP/6-311++G(d,p) and LANL2DZ levels. The predicted vibrational frequencies are in good agreement with the experimental values. The TDDFT calculations lead to a close agreement with the experimental absorption spectra in solvent media. Molecular orbital coefficients analyses reveal that the electronic transitions are mainly assigned to $\pi \rightarrow \pi^*$ for heipeoH and mixed LLCT, LMCT and MLCT for the complexes. This systematic study may be useful for the analysis of the spectroscopic behavior of coordination compounds of other imineoximes.

Acknowledgment

This work is a part of a research project OUAP(F)-2012/12. We thank Uludag University for the financial support given to the project.

Appendix A. Supplementary material

CCDC 956193–956195 contain the supplementary crystallographic data for this paper. These data can be obtained free of charge from The Cambridge Crystallographic Data Centre via www.ccdc.cam.ac.uk/data_request/cif.

Appendix B. Supplementary data

Supplementary data related to this article can be found at <http://dx.doi.org/10.1016/j.jorgchem.2013.12.011>.

References

- [1] K. Karljiković, B. Stanković, Z. Binenfeld, *Mikrochim. Acta* 2 (1985) 195.
- [2] M.A. Kabil, M.A. Akl, M.E. Khalifa, *Anal. Sci.* 15 (1999) 433.
- [3] A.M. Sastre, J. Szymanowski, *Solvent Extr. Ion Exch.* 22 (2004) 737.
- [4] B. Dede, F. Karipcin, M. Cengiz, *J. Chem. Sci.* 121 (2009) 163.
- [5] A. Shokrollahi, M. Ghaedi, H. Ghaedi, *J. Chin. Chem. Soc.* 54 (2007) 933.
- [6] A. Chakravorty, *Coord. Chem. Rev.* 13 (1974) 1.
- [7] A.B. Packard, J.F. Kronauge, P.J. Day, S.T. Treves, *Nucl. Med. Biol.* 25 (1998) 531.
- [8] E. Zangrando, M. Trani, E. Stabon, C. Carfagna, B. Milani, G. Mestroni, *Eur. J. Inorg. Chem.* (2003) 2683.
- [9] H. Nakamura, Y. Iitaka, H. Sakakibara, H. Umezawa, *J. Antibiot.* 27 (1974) 894.
- [10] H.A. Kirst, E.F. Szymanski, D.E. Doman, J.L. Ocolowicz, N.D. Jones, M.O. Chaney, R.L. Hamill, M.M. Hoehn, *J. Antibiot.* 28 (1975) 286.
- [11] V.V. Ponomareva, N.K. Dalley, X. Kou, N.N. Gerasimchuk, K.V. Domasevich, *J. Chem. Soc. Dalton Trans.* (1996) 2351.
- [12] T.W. Hambley, E.C.H. Ling, S. O'Mara, M.J. McKeage, P.J. Russell, *J. Biol. Inorg. Chem.* 5 (2000) 675.
- [13] A.G. Quiroga, L. Cubo, E. de Blas, P. Aller, C.J. Navarro-Ranninger, *Inorg. Biochem.* 101 (2007) 104.
- [14] S. Zorbas-Seifried, M.A. Jakupec, N.V. Kukushkin, M. Groessl, Ch.G. Hartinger, O. Semenova, H. Zorbas, V.Yu. Kukushkin, B.K. Kepler, *Mol. Pharmacol.* 71 (2007) 357.
- [15] Y.Yu. Scaffidi-Domianello, K. Meelich, M.A. Jakupec, V.B. Arion, V.Yu. Kukushkin, M. Galanski, B.K. Kepler, *Inorg. Chem.* 49 (2010) 5669.
- [16] R.S. Lokhande, V.R. Patil, P.P. Shevde, S.M. Lele, *Int. J. Chem. Sci.* 8 (2010) 88.
- [17] P. Jayaseelan, S. Prasad, S. Vedanayaki, R. Rajavel, *Eur. J. Chem.* 2 (2011) 480.
- [18] E.C.H. Ling, G.W. Allen, K. Vickery, T.W. Hambley, *J. Inorg. Biochem.* 78 (2000) 55.
- [19] N.I. Dodoff, M. Kubiak, J. Kuduk-Jaworska, A. Mastalarz, A. Kochel, V. Vassilieva, N. Vassilev, N. Trendafilova, I. Georgieva, M. Lalia-Kantouri, M. Apostolova, *Chemija* 20 (2009) 208.
- [20] Z. Xu, L. Zhou, *Int. J. Quantum. Chem.* 111 (2011) 1907.
- [21] K. Malek, M. Vala, H. Kozłowski, L.M. Proniewicz, *Magn. Reson. Chem.* 42 (2004) 23.
- [22] R.M. Jones, M.J. Goldcamp, J.A. Krause, M.J. Baldwin, *Polyhedron* 25 (2006) 3145.
- [23] I. Georgieva, N. Trendafilova, G. Bauer, *Spectrochim. Acta A* 63 (2006) 403.
- [24] K.V. Luzyanin, V.Yu. Kukushkin, M.L. Kuznetsov, A.D. Ryabov, M. Galanski, M. Haukka, E.V. Tretyakov, V.I. Ovcharenko, M.N. Kopylovich, A.J.L. Pombeiro, *Inorg. Chem.* 45 (2006) 2296.
- [25] M. Lalia-Kantouri, C.D. Papadopoulos, M. Quirós, A.G. Hatzidimitriou, *Polyhedron* 26 (2007) 1292.
- [26] M.A. Palacios, A.J. Mota, J.E. Perea-Buceta, F.J. White, E.K. Brechin, E. Colacio, *Inorg. Chem.* 49 (2010) 10156.
- [27] K. Serbest, K. Karaoglu, M. Erman, M. Er, I. Degirmencioglu, *Spectrochim. Acta A* 77 (2010) 643.
- [28] V.A. Shagun, A.M. Vasil'tsov, A.V. Ivanov, A.I. Mikhaleva, B.A. Trofimov, *J. Struct. Chem.* 54 (2013) 17.
- [29] T. Stepanenko, L. Lapinski, M.J. Nowak, L. Adamowicz, *Vib. Spectra* 26 (2001) 65.
- [30] K. Sohlberg, K.D. Dobbs, *J. Mol. Struct. (Theochem)* 577 (2002) 137.
- [31] F.F. Jian, P.S. Zhao, Z.S. Bai, L. Zhang, *Struct. Chem.* 16 (2005) 635.
- [32] B. Golec, Z. Mielke, *J. Mol. Struct.* 844–845 (2007) 242.
- [33] B. Golec, J. Grzegorzec, Z. Mielke, *Chem. Phys.* 353 (2008) 13.
- [34] T. Irshaidat, *Tetrahedron Lett.* 49 (2008) 631.
- [35] M. Kurt, T.R. Sertbakan, M. Ozduran, *Spectrochim. Acta A* 70 (2008) 664.
- [36] N.V. Istomina, N.A. Shcherbina, L.B. Krivdin, *Russ. J. Org. Chem.* 45 (2009) 481.
- [37] H. Tanak, F. Ersahin, Y. Koysal, E. Agar, S. Isik, M. Yavuz, *J. Mol. Model.* 15 (2009) 1281.
- [38] A.A. Agar, H. Tanak, M. Yavuz, *Mol. Phys.* 108 (2010) 1759.
- [39] V. Arjunan, C.V. Mythili, K. Mageswari, S. Mohan, *Spectrochim. Acta A* 79 (2011) 245.
- [40] N.R. Gonerwar, V.B. Jadhav, K.D. Jadhav, R.G. Sarawadekar, *Res. Pharm.* 2 (2012) 18.
- [41] Y. Kaya, V.T. Yilmaz, T. Arslan, O. Buyukgungor, *J. Mol. Struct.* 1024 (2012) 65.
- [42] Y. Kaya, C. Icel, V.T. Yilmaz, O. Buyukgungor, *Spectrochim. Acta A* 108 (2013) 133.
- [43] Y. Kaya, V.T. Yilmaz, *Struct. Chem.*, <http://dx.doi.org/10.1007/s11224-013-0273-6>.
- [44] G.M. Sheldrick, *Acta Crystallogr. A* 64 (2008) 112.
- [45] A.D. Becke, *J. Chem. Phys.* 98 (1993) 5648.
- [46] M.J. Frisch, G.W. Trucks, H.B. Schlegel, G.E. Scuseria, M.A. Robb, J.R. Cheeseman, J.A. Montgomery Jr., T. Vreven, K.N. Kudin, J.C. Burant, J.M. Millam, S.S. Iyengar, J. Tomasi, V. Barone, B. Mennucci, M. Cossi, G. Scalmani, N. Rega, G.A. Petersson, H. Nakatsuji, M. Hada, M. Ehara, K. Toyota, R. Fukuda, J. Hasegawa, M. Ishida, T. Nakajima, Y. Honda, O. Kitao, H. Nakai, M. Klene, X. Li, J.E. Knox, H.P. Hratchian, J.B. Cross, V. Bakken,

- C. Adamo, J. Jaramillo, R. Gomperts, R.E. Stratmann, O. Yazyev, A.J. Austin, R. Cammi, C. Pomelli, J.W. Ochterski, P.Y. Ayala, K. Morokuma, G.A. Voth, P. Salvador, J.J. Dannenberg, V.G. Zakrzewski, S. Dapprich, A.D. Daniels, M.C. Strain, O. Farkas, D.K. Malick, A.D. Rabuck, K. Raghavachari, J.B. Foresman, J.V. Ortiz, Q. Cui, A.G. Baboul, S. Clifford, J. Cioslowski, B.B. Stefanov, G. Liu, A. Liashenko, P. Piskorz, I. Komaromi, R.L. Martin, D.J. Fox, T. Keith, M.A. Al-Laham, C.Y. Peng, A. Nanayakkara, M. Challacombe, P.M.W. Gill, B. Johnson, W. Chen, M.W. Wong, C. Gonzalez, J.A. Pople, Gaussian 03, Revision E.01, Gaussian, Inc., Wallingford, CT, 2004.
- [47] H.A. Dabbagh, A. Teimouri, A.N. Chermahini, M. Shahraki, *Spectrochim. Acta A* 69 (2008) 449.
- [48] N. Sundaraganesan, S. Illakiamani, H. Saleem, P.M. Wojciechowski, D. Michalska, *Spectrochim. Acta A* 61 (2005) 2995.
- [49] A.J.L. Jesus, M.T.S. Rosado, I. Reva, R. Fausto, M.E. Eusebio, J.S. Redinha, *J. Phys. Chem. A* 110 (2006) 4169.
- [50] H. Yoshida, A. Ehara, H. Matsuura, *Chem. Phys. Lett.* 325 (2000) 477.
- [51] H. Yoshida, K. Takeda, J. Okamura, A. Ehara, H. Matsuura, *J. Phys. Chem. A* 106 (2002) 3580.
- [52] R. Dennington, T. Keith, J. Millam, K. Eppinnett, W.L. Hovell, R. Gilliland, GaussView, Version 3.07, Semichem Inc., Shawnee Mission, KS, 2003.
- [53] M.H. Jamróz, *Vibrational Energy Distribution Analysis VEDA 4*, Warsaw, 2004.
- [54] K. Wolinski, J.F. Hinton, P. Pulay, *J. Am. Chem. Soc.* 112 (1990) 8251.
- [55] N.M. O'Boyle, A.L. Tenderholt, K.M. Langner, *J. Comput. Chem.* 29 (2008) 839.
- [56] D.W. Phelps, W.F. Little, D.J. Hodgso, *Inorg. Chem.* 15 (1976) 2263.
- [57] M.S. Hussain, E.O. Schlemper, *Inorg. Chem.* 18 (1979) 1116.
- [58] A.D. Ryabov, G.M. Kazankov, A.K. Yatsimirsky, L.G. Kuz'mina, O.Yu. Burtseva, N.V. Dvortsova, V.A. Polyakov, *Inorg. Chem.* 31 (1992) 3083.
- [59] C.K. Pal, S. Chattopadhyay, C. Sinha, A. Chakravorty, *Inorg. Chem.* 35 (1996) 2442.
- [60] V.Yu. Kukushkin, T. Nishioka, D. Tudela, K. Isobe, I. Kinoshita, *Inorg. Chem.* 36 (1997) 6157.
- [61] K. Selvakumar, S. Vancheesan, B. Varghese, *Polyhedron* 16 (1997) 2257.
- [62] A. Audhya, K. Bhattacharya, M. Maity, M. Chaudhury, *Inorg. Chem.* 49 (2010) 5009.
- [63] B. Guhathakurta, C. Biswas, J.P. Naskar, L. Lu, M. Zhu, *J. Chem. Crystallogr.* 41 (2011) 1355.
- [64] J. Grzegorzec, Z. Mielke, *Eur. J. Org. Chem.* (2010) 5301.
- [65] A.R. Bekhradnia, S. Arshadi, *Monatsh. Chem.* 138 (2007) 725.
- [66] O. Alver, M.F. Kaya, M. Bilge, C. Parlak, *J. Theor. Chem* 2013 (2013) 10.
- [67] K. Malek, H. Kozłowski, L.M. Proniewicz, *Polyhedron* 24 (2005) 1175.
- [68] M.E. Keeney, K. Osseo-Asare, K.A. Woode, *Coord. Chem. Rev.* 59 (1984) 141.
- [69] N.V. Thakkar, B.C. Haldar, *J. Inorg. Nucl. Chem.* 42 (1980) 843.
- [70] M. Carcelli, P. Cozzini, R. Marroni, P. Pelagatti, C. Pelizzi, P. Sgarabotto, *Inorg. Chim. Acta* 285 (1999) 138.
- [71] D.J. Giesen, N. Zumbulyadis, *Phys. Chem. Chem. Phys.* 4 (2002) 5498.
- [72] A. El Moncef, E. Zaballos, R.J. Zaragoza, *Tetrahedron* 67 (2011) 3677.
- [73] A.E. Reed, R.B. Weinstock, F. Weinhold, *J. Chem. Phys.* 83 (1985) 735.
- [74] A.E. Reed, L.A. Curtiss, F. Weinhold, *Chem. Rev.* 88 (1988) 899.